ONLINE AND OFFLINE EVENT SELECTIONS FOR UPC HEAVY-FLAVOUR AND JET EVENTS WITH CMS*

Balázs Csaba Kovács

on behalf of the CMS Collaboration

Eötvös Loránd University, Budapest, Hungary

Received 11 December 2024, accepted 23 December 2024, published online 6 March 2025

In this contribution, we present the experimental techniques developed to select good photo-nuclear events in ultraperipheral heavy-ion collisions (UPCs) with the CMS detector at the Large Hadron Collider (LHC). The CMS Collaboration has recently designed and implemented a new trigger strategy to maximize the number of collected photo-nuclear events in Pb+Pb UPCs. This goal was achieved by integrating the Zero Degree Calorimeters (ZDCs) in the Level-1 trigger system of CMS and by triggering on events based on the presence of forward neutrons in the ZDCs. Therefore, we could select events where only one of the colliding nuclei breaks up while the other one stays intact. A rapidity gap selection, based on the information provided by the hadron forward calorimeters (HFs) was also applied in the direction of the outgoing photon. The presented techniques were used in the first measurement of the D^0 production in Pb+Pb UPC collisions at $\sqrt{s_{NN}} = 5.36$ TeV.

DOI:10.5506/APhysPolBSupp.18.1-A46

1. Introduction

Heavy-flavour photoproduction in ultraperipheral heavy-ion collisions provides a clean experimental environment for studying cold, high-density nuclear matter. Theoretical calculations based on the factorization limit of quantum chromodynamics (QCD) use parton distribution functions (PDFs) to describe the partonic structure of matter inside the nucleus or the proton. These PDFs are considered to be independent of the specific hard-scattering process, however, they can only be extracted from global fits to experimental data. The PDFs are usually treated as a function of the momentum fraction

* Presented at the Diffraction and Low-x 2024 Workshop, Trabia, Palermo, Italy, 8–14 September, 2024.

(Bjorken-x) of the parton and the nucleus (or proton), and the virtuality (Q^2) of the hard-scattering. The evolution of PDFs between different x and Q^2 values can be described by QCD evolution equations. The nature of evolution equations at very low-x is, however, still unknown and the predicted emergence of a non-linear regime of evolution equations (saturation) is yet to be confirmed by experimental data.

The main advantage of studying heavy-flavour hadron production is that we can scan a wide region of the x and Q^2 space, while also staying within the range, where perturbative QCD calculations can describe heavy-quark production even at $p_{\mathrm{T}} = 0$ GeV. The impact parameter in ultraperipheral collisions (UPCs) is greater than twice the radius of the nucleus. In these events, the leading order (direct) process of D^0 meson production is a scattering between a quasi-real photon from one nucleus and a gluon from the other nucleus. A c–$\bar{c}$ (or b–$\bar{b}$) quark pair is produced from the scattering, and the D^0 mesons (and their anti-particles) are produced in the hadronization of such quarks. After the interaction, the photon-emitting nucleus stays intact, while the other nucleus breaks up. Based on the details of the scattering process, we can differentiate events containing direct or resolved photons, the latter case being, when the photon virtually fluctuates before interacting with the gluon. Our goal was designing a selection that provides the highest selection efficiency for both direct and resolved events, while minimizing the contamination coming from hadronic events.

2. The CMS detector

The central feature of the CMS apparatus is a superconducting solenoid of 6 m internal diameter, providing a magnetic field of 3.8 T. Within the solenoid volume, there are a silicon pixel and strip tracker, a lead tungstate crystal electromagnetic calorimeter (ECAL), and a brass and scintillator hadron calorimeter (HCAL), each composed of a barrel and two endcap sections. Forward calorimeters extend the pseudorapidity coverage provided by the barrel and endcap detectors. The two halves of the Forward Hadron (HF) calorimeter are located 11.2 m from the interaction region, one on each end, and together they provide coverage in the range of $3.0 < |\eta| < 5.2$. Energy measurement of very forward neutrons is possible by the Zero Degree Calorimeters (ZDCs). The ZDCs are located in the neutral particle absorber, roughly 140 m from the CMS interaction point, between the two beampipes. These detectors can measure the energy of neutral particles in the pseudorapidity range of $|\eta| > 8.5$, since charged particles are deflected by dipole magnets before reaching the ZDCs. Events of interest are selected using a two-tiered trigger system. The first level (L1), composed of custom hardware processors, uses information from the calorimeters and muon detectors to select events at a rate of around 100 kHz within a fixed latency of

4 μs [1]. The second level, known as the high-level trigger (HLT), consists of a farm of processors running a version of the full event reconstruction software optimized for fast processing, and reduces the event rate to around 1 kHz before data storage [2]. More detailed descriptions of the CMS detector, together with a definition of the coordinate system used and the relevant kinematic variables, can be found in Refs. [3, 4].

3. Trigger strategy for photoproduction with CMS

This work uses the Pb+Pb dataset recorded in 2023 at the nucleon–nucleon center-of-mass energy of $\sqrt{s_{NN}} = 5.36$ TeV, with an integrated luminosity of about 1.38 nb^{-1}. We have developed new trigger algorithms for 2023 to maximize the collected statistics of UPC photo-nuclear events. The main improvement from previous years was the integration of the ZDCs into the L1 trigger. This enabled us to use a combination of signals from the ZDCs and the central calorimeters to make the L1 decision.

To select D^0 mesons, we used different triggers depending on the transverse-momentum (p_{T}) of the meson. For D^0 mesons with $p_{\mathrm{T}} > 5$ GeV, we required that one of the ZDCs has a signal below the 1 neutron ($1n$) threshold energy, while the other ZDC has a signal above this threshold (ZDC XOR). In addition, an L1-jet with energy above 8 GeV was required. In the $2 < D^0 p_{\mathrm{T}} < 5$ GeV region, we only required one of the ZDC signals to be below the $1n$ threshold with no jet condition (ZDC OR), hence selecting collisions with no forward neutrons on one side. This looser condition at low p_{T} was necessary since jet reconstruction is very inefficient in this region.

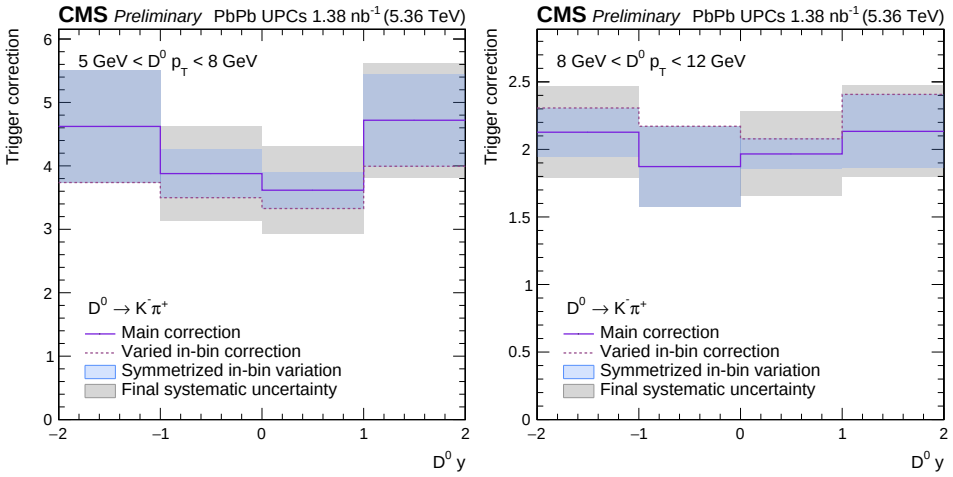

Fig. 1. Jet trigger corrections ($1/\varepsilon_{\mathrm{trigger}}$) as a function of D^0 p_{T} and rapidity in events, where the broken nucleus went in the negative z direction.

The trigger efficiency of the ZDC conditions was found to be above 99%, which was evaluated based on the ZDC signal distribution in empty bunch crossing events. The jet trigger efficiencies were calculated by a data-driven method in bins of D^0 p_{T} and D^0 y, the trigger corrections ($1/\varepsilon_{\mathrm{trigger}}$) can be seen in Fig. 1.

4. Offline event selection

The two main components of the offline selections were the ZDC selection and the rapidity-gap condition. The offline ZDC selection was a tighter version of the previously described ZDC XOR condition. The rapidity gap meant that we required that there were no particle-flow candidates above a given energy threshold (9.2 GeV for HF+, 8.6 GeV for HF−) in the pseudorapidity coverage of the HF on the side of the detector with no neutrons in the ZDC. The energy threshold of this gap was chosen to be above the noise level of the HF, while also low enough not to influence the fraction of direct and resolved photon events in the sample, since resolved photon events can leave more energy in this forward region compared to direct photon events. The rapidity gap condition significantly reduced the hadronic contamination in our data samples, its effect can be seen in Fig. 2. Events failing the gap condition have a high-multiplicity tail characteristic to hadronic events, while for passing events the distribution peaks at lower values.

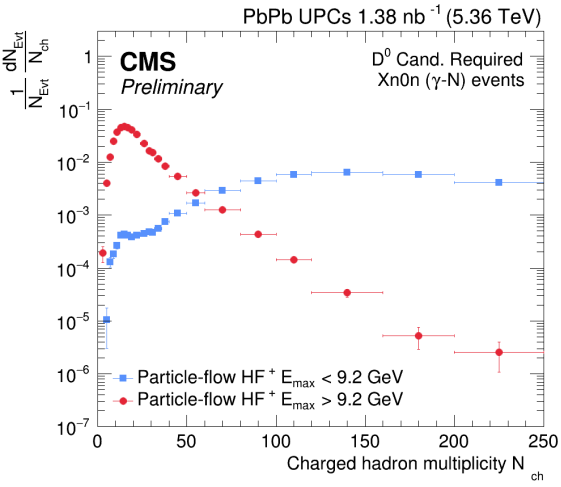

Fig. 2. Multiplicity distribution of charged tracks satisfying a high-purity cut for events passing all selections, with at least one selected D^0 meson with $2 < p_{\mathrm{T}} < 12$ GeV. Events passing the rapidity gap condition are shown in red, failing ones are shown in blue.

Besides the two conditions already mentioned, we also required events to have at most three reconstructed vertices. This was useful since we used a reconstruction algorithm optimized for low-multiplicity UPCs, which would lead to vertex splitting in high-multiplicity hadronic events. In addition, a Missing Transverse Energy (MET) filter [5] was also applied in order to reject beam-gas and machine-induced background events.

The efficiency of the offline selections was calculated by the percentage of passing events in Monte Carlo (MC) simulations. These events were generated by the PYTHIA 8 [6] event generator and D^0-meson decays were simulated with EvtGen 2.0.0 [7]. The events were propagated through the CMS detector with the Geant4 [8] package. The offline selection efficiencies were above 98% in almost all regions, the main efficiency loss resulted from the cuts on the maximum number of vertices and the rapidity gap condition.

5. D^0 meson reconstruction and selection

The D^0 mesons in selected events were reconstructed using their daughter particles. We only considered the $D^0 \to K^-\pi^+$ decay channel, therefore the D^0 mesons were reconstructed from oppositely charged, "high-purity" [9] track pairs, whose combined invariant mass fell within 0.2 GeV/c^2 of the world-average D^0 mass [10]. Only tracks with $|\eta| < 2.4$ and $p_T > 1$ GeV were used. The reconstructed D^0 mesons had to satisfy multiple geometrical conditions, a similar strategy was implemented as in Ref. [11]. These conditions included a minimum χ^2 value for the reconstruction of the secondary vertex, a maximum angle between the momentum of the daughter tracks, and a maximum angle between the total momentum of the meson and the vector pointing from the primary to the secondary vertex. Furthermore, we required a minimum value for the distance between the primary and secondary vertices ("decay length") divided by its own uncertainty.

The selection efficiency of D^0 mesons was evaluated using the same MC simulations that were described in the previous section. The D^0 selection efficiency values increased with D^0 p_T and were overall in the 5–30% range. This efficiency for non-prompt D^0 mesons was observed to be significantly larger compared to prompt processes, which could be explained by non-prompt ($b \to D^0$) candidates having large decay lengths.

6. Summary

We have successfully implemented and presented multiple selection criteria for selecting heavy-ion UPC events containing D^0 mesons. These procedures included both online (trigger) and offline (event and D^0 candidate) selections. Events with a filled ZDC on one side and an empty ZDC on the

other side were selected. In addition, a rapidity gap with no high-energy particles inside was also required. The described methods were used in the first measurement of D^0 production in Pb+Pb UPC events at $\sqrt{s_{NN}} = 5.36$ TeV. In the future, these techniques could be used to study heavy-flavour hadron and jet production in heavy-ion UPC events at the LHC.

Supported by the National Research, Development and Innovation Office (NKFIH) research grant K 146913 and the EKÖP-24 University Excellence Scholarship Program of the Ministry for Culture and Innovation from the source of the National Research, Development and Innovation Fund.

REFERENCES

[1] CMS Collaboration (A.M. Sirunyan *et al.*), *J. Instrum.* **15**, P10017 (2020).
[2] CMS Collaboration (V. Khachatryan *et al.*), *J. Instrum.* **12**, P01020 (2017).
[3] CMS Collaboration (S. Chatrchyan *et al.*), *J. Instrum.* **3**, S08004 (2008).
[4] CMS Collaboration (A. Hayrapetyan *et al.*), *J. Instrum.* **19**, P05064 (2024).
[5] CMS Collaboration (A.M. Sirunyan *et al.*), *J. Instrum.* **14**, P07004 (2019).
[6] C. Bierlich *et al.*, arXiv:2203.11601 [hep-ph].
[7] D.J. Lange, *Nucl. Instrum. Methods Phys. Res. A* **462**, 152 (2001).
[8] S. Agostinelli *et al.*, *Nucl. Instrum. Methods Phys. Res. A* **506**, 250 (2003).
[9] CMS Collaboration, *J. Instrum.* **9**, P10009 (2014).
[10] S. Navas *et al.*, *Phys. Rev. D* **110**, 030001 (2024).
[11] CMS Collaboration (A.M. Sirunyan *et al.*), *Phys. Lett. B* **782**, 474 (2018).